A Study of the Reduction Mechanism of *p*-Dimethylaminobenzaldehyde to 1,2-Bis(*p*-dimethylaminophenyl)-1,2-ethanediol by Rotating Disk Electrode Voltammetry

Isao TANIGUCHI,* Kazuo YASUKOUCHI, Akiko YOSHIYAMA,† and Taro SEKINE†

Department of Industrial Chemistry, Faculty of Engineering, Kumamoto University, 2-39-1, Kurokami, Kumamoto 860

†*Department of Electronic Chemistry, Graduate School at Nagatsuta, Tokyo Institute of Technology, 4259, Nagatsuta, Midori-ku, Yokohama 227*

(Received August 22, 1978)

Rotating disk electrode voltammetry was applied to study the reduction mechanism of *p*-dimethylaminobenzaldehyde (**1**) in water–ethanol alkaline solutions by using a mercury-plated platinum rotating disk electrode. In the logarithmic analysis of the wave, the plots of log $[i^{2/3}/(i_d-i)]$ *vs.* E showed good linearity, and the shifts of the half-wave potential with an increase in the rotation speed of the electrode (ω) and in the initial concentration of **1** (C) were $\partial E_{1/2}/\partial \log \omega = -22 \pm 2$ mV and $\partial E_{1/2}/\partial \log C = 19 \pm 2$ mV, respectively. On the other hand, no appreciable change in $E_{1/2}$ was observed with varying alkalinities of the solutions. These results and the large shift of $E_{1/2}$ with an increase in the concentration of water ($\partial E_{1/2}/\partial \log[H_2O] = ca.$ 50 mV) are explained in terms of the following reactions:

$$R + e \rightleftarrows R^{\cdot} \text{ (solvated by water)}, \quad (1)$$

$$2R^{\cdot} \xrightarrow{k} D^{2-} \text{ (r.d.s.)}, \quad (2)$$

$$D^{2-} + 2H_2O \longrightarrow DH_2 + 2OH^-, \quad (3)$$

where R and $R^{\cdot}$ are the molecule and the radical of **1**, respectively, D^{2-} is the dimer of $R^{\cdot}$ and DH_2 is the hydrodimer (**2**) of R. The rate of the dimerization reaction (k in Eq. 2) was estimated to be 2.5×10^4 M^{-1} s^{-1} from the shift of $E_{1/2}$ with log ω for the 50% water–ethanol solution containing 1 M NaOH, and this rate constant decreased with decreasing water concentration.

Rotating disk electrode voltammetry (RDEV) is one of the most useful techniques for studying an electrode reaction. It is more advantageous than polarography using a dropping-mercury electrode because (i) the rotation speed of the electrode can be varied over a wide range, whereas the variation of the drop-time is limited, and (ii) even in a high concentration of a reactant the current-potential curve at an RDE can be obtained and the reaction mechanism may be examined under conditions similar to those for a macro-scale electrolytic synthesis. Furthermore, recently Saveant *et al.* have reported[1,2] the theoretical relationship between current and potential at a rotating disk electrode (RDE) and have given some diagnostic criteria for determining the correct mechanism among various types of hydrodimerization reactions coupled to an electron transfer.

On the other hand, Allen reported[3] that *p*-dimethylaminobenzaldehyde (**1**) was reduced to 1,2-bis(*p*-dimethylaminophenyl)-1,2-ethanediol (**2**) (the mixture of *dl* and *meso* types) in a water–alcohol solution of KOH with a mercury electrode at −1.9 V (*vs.* NCE) in 97% yield. However, no report has been published for the reduction mechanism. Thus, to clarify the reaction pathway, RDEV was applied for the reduction of **1** to **2** in alkaline solutions at a mercury-plated rotating disk electrode (MPRDE).

Experimental

The voltammograms were measured using a set of apparatuses for RDEV (Nikko Keisoku RRD-1, SC-2, NPS-2, and NPGS-1) and an X-Y recorder (Riken D-72BP). The electrolytic cell (NKC-1) and the platinum rotating disk electrode (PRDE) were also constructed by Nikko Keisoku. The MPRDE (r=0.302 cm) was prepared for each set of runs as follows: The PRDE was first polarized cathodically at 5 mA and at the rotation speed of the electrode of 104.7 rad s^{-1} for 10 min in a copper sulfate solution used commonly for a copper coulometer, and then the copper-plated platinum electrode was dipped into a saturated $Hg(NO_3)_2$ solution for 30 s. The MPRDE thus prepared was set into the apparatus immediately after being washed with distilled water.

The test solution was a 1 M NaOH solution containing 50 % v/v ethanol, unless stated otherwise, and the solution was deaerated by bubbling with purified nitrogen. The measurements were carried out at 25±0.5 °C under continuous flow of nitrogen over the solution surface. The rate of potential sweep used was 16.7 mV s^{-1}. The reference electrode was a saturated calomel electrode (SCE); the potentials given in this paper are referred to this electrode without any correction the liquid junction potential. The value of the half-wave potential adopted is the average of values obtained by several experiments. The uncertainty is within ±3 mV. The kinematic viscosity (ν) of the solution (0.0331 cm^2 s^{-1} for a 1 M NaOH solution containing 50% v/v ethanol) was measured by using a viscometer (Shibata SF 7741). The diffusion coefficient (D) of **1** (3.09×10^{-6} cm^2 s^{-1}) was determined by using the Levich equation, and this value was also assumed to be valid for the diffusion coefficient of the anion radical of **1**.

The macro-scale electrolyses were carried out in 100 ml of 1 M NaOH water–ethanol solutions containing 1 g (67 mM) of **1** by controlling the cathode potential at −1.8 V *vs.* SCE. An H-type electrolytic cell, which is the same as that described elsewhere,[4] was used. The cathode was a mercury pool (20 cm^2) and the anode was a platinum plate (4 cm^2). During electrolysis, one electron/molecule of **1** was consumed. After reduction, the products were separated into *dl* and *meso* types of **2** by Allen's method,[3] and were weighed to determine the *dl*/*meso* ratio. After electrolysis, *meso*-**2** was always obtained from 50 % water–ethanol solution, by adding water when necessary. The total yield of the products was *ca.* 70%.

The diastereomers were identified by means of both their NMR spectra[5] (100 MHz at room temperature) and melting points.[3] The characteristics obtained are:
dl; mp 113 °C, NMR (DMSO-d_6) δ=5.0 (2H, s, hydroxylic),
meso; mp 178 °C, NMR (DMSO-d_6) δ=4.76 (2H, s, hydroxylic).

All reagents used were analytical GR grade without further purification. Throughout this paper 1 M=1 mol dm^{-3}.

Results

The voltammograms for the reduction of **1** at the MPRDE were measured in water–ethanol alkaline solutions by changing the rotation speed of the electrode (ω), the initial concentration of **1** (C), and the alkalinity of the solution. The results are shown in Figs. 1—4. In the logarithmic analysis of the wave (Fig. 1), the relationship between log $[i^{2/3}/(i_d-i)]$ and the cathode potential (E) shows good linearity, with the slope of the line being 57±3 mV (the plots of log $[i/(i_d-i)]$ *vs.* E are also shown for comparison in Fig. 1). The half-wave potential ($E_{1/2}$) shifted to more negative potentials with increasing ω ($\partial E_{1/2}/\partial \log \omega = -22\pm2$ mV, see Fig. 2) and to more positive potentials with increasing C ($\partial E_{1/2}/\partial \log C = 19\pm2$ mV, see Fig. 3). On the other hand, no appreciable change in $E_{1/2}$ was observed with alkalinity of the solution (Fig. 4), when we take into account the liquid junction potential (from the Henderson equation, the liquid junction potentials between the test solution and the saturated KCl solution are: 8.5 mV (1 M NaOH), 0.44 mV (0.1 M NaOH+0.9 M $NaClO_4$), and 0.01 mV (0.01 M NaOH+0.99 M $NaClO_4$)).

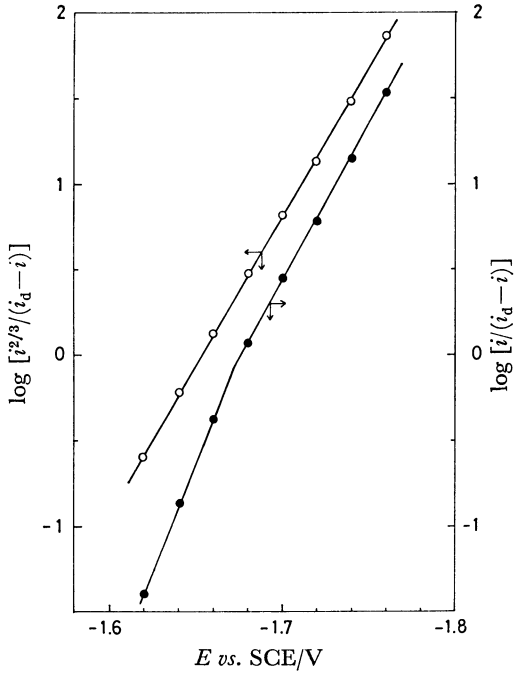

Fig. 1. Logarithmic analysis of the wave for 9.7 mM of **1** at ω=261.8 rad s^{-1}.

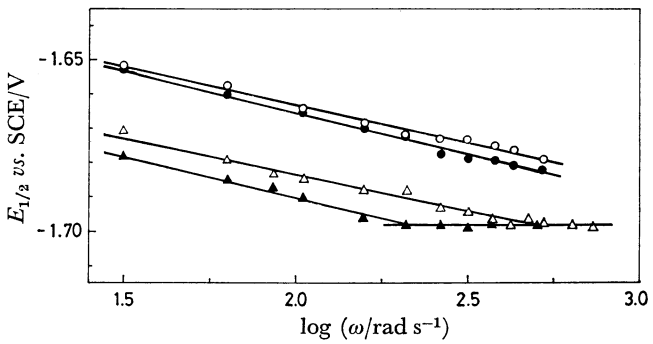

Fig. 2. Variations of half-wave potential as a function of the rotation speed of the electrode at various concentrations of **1**; ○: 15.7 mM, ●: 9.71 mM, △: 1.19 mM, ▲: 0.406 mM.

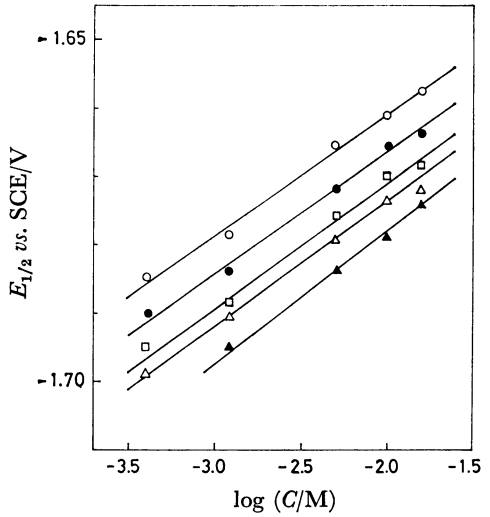

Fig. 3. Variations of half-wave potential as a function of the concentration of **1** at various rotation speeds of the electrode; ○: 62.8 rad s^{-1}, ●: 104.7 rad s^{-1}, □: 157.1 rad s^{-1}, △: 209.4 rad s^{-1}, ▲: 314.2 rad s^{-1}.

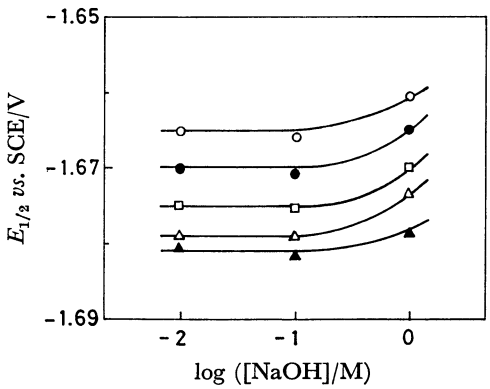

Fig. 4. Variations of half-wave potential as a function of NaOH concentration at various rotation speeds of the electrode; ○: 62.8 rad s^{-1}, ●: 104.7 rad s^{-1}, □: 157.1 rad s^{-1}, △: 209.4 rad s^{-1}, ▲: 314.2 rad s^{-1}. [**1**]=10 mM. The ionic strength and sodium ion concentration were maintained constant (1 M) by adding $NaClO_4$ crystals.

Discussion

Reduction Mechanism. The results shown in Fig. 1 indicate that the reduction of **1** is successfully explained

in terms of Eq. 13 in the appendix of the present paper, for $n=1$. This mechanism is also consistent with the facts that (i) the n-value (electrons consumed/molecule of **1**) obtained by coulometry was one, (ii) **2** was produced by controlled-potential electrolysis, and (iii) the dependences of $E_{1/2}$ on both ω and C were in good agreement with those estimated by Eq. 14 in the appendix. Thus, when we take into account the diagnostic criteria (see Tables 3 and 4 in Ref. 2), **1** was reduced by

$$R + e \rightleftharpoons R^{\cdot -}, \quad (1)$$

$$2R^{\cdot -} \longrightarrow D^{2-} \text{ (r.d.s.)}, \quad (2)$$

$$D^{2-} + 2H_2O \longrightarrow DH_2 + 2OH^-, \quad (3)$$

where R and $R^{\cdot -}$ are the molecule and the anion radical of **1**, respectively, D is the dimer of R, and thus DH_2 is the hydrodimer (**2**). It should be noted that, as is shown by Eq. 2, the dimerization reaction occurred between two anion radicals of **1**.

For dimerization reactions, (i) the coupling between two anion radicals (DIM I mechanism) has been excluded because of the coulombic repulsive force between the radicals, and the coupling between an anion radical and a neutral radical produced by a protonation to the anion radical (DIM II mechanism) has generally been considered to be the predominant reaction in aqueous alkaline solutions, and (ii) in a non-aqueous medium without proton-donating reagents, an ion-pair formation of an anion radical with the cation of a supporting electrolyte (DIM III mechanism) has been reported to be important for the coupling reaction. Both these considerations were examined. For the DIM II mechanism, $E_{1/2}$ must vary in 19.7 mV/pH (in fact, for the reduction of benzaldehyde, $E_{1/2}$ shifts in this manner[6]), but in the present experiment, since no appreciable change in $E_{1/2}$ was observed with alkalinity of the solution (see Fig. 4), the DIM II mechanism must be rejected. When the anion radical forms an ion-pair with the cation of a supporting electrolyte, $E_{1/2}$ is affected by the concentration and the kind of the cation. Thus the variation of $E_{1/2}$ was tested by changing the supporting electrolyte. No appreciable difference in $E_{1/2}$ was observed when either 0.1 M tetraethylammonium hydroxide or 0.1 M sodium hydroxide was used as a supporting electrolyte.

According to recent developments in the study of ion-pair formations,[7,8] not only does an anion radical form a contact ion-pair ($R^{\cdot -}/M^+$, where M^+ is the cation of a supporting electrolyte), but an anion radical interacts with water molecules; thus solvation ($R^{\cdot -}/H_2O$) and/or a separated ion-pair ($R^{\cdot -}/H_2O/M^+$) formation are to be considered when water concentration is greater than 1 M. In both cases the electric repulsion between anion radicals diminishes. Recently, Lamy *et al.*[9] have concluded from the results obtained by linear sweep voltammetry that for the electrohydrodimerization of activated olefines, the coupling of two anion radicals solvated by water molecule was the most probable reaction in a low acidity media.

The effect of water concentration of $E_{1/2}$ was then examined. The $E_{1/2}$ shifted to a more negative potential with a decrease in the concentration of water (Fig. 5).

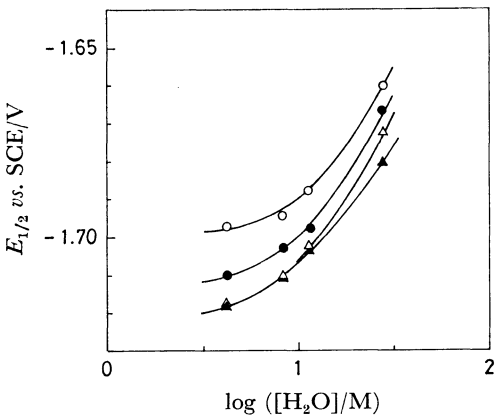

Fig. 5. Variations of half-wave potential as a function of water concentration in 1 M NaOH water–ethanol solutions containing 10 mM of **1** at various rotation speeds of the electrode; ○: 62.8 rad s^{-1}, ●: 104.7 rad s^{-1}, △: 209.4 rad s^{-1}, ▲: 314.2 rad s^{-1}.

Though the shift of $E_{1/2}$ may include the variation of the liquid junction potential which results from the change of the composition of the test solution, the large shift of $E_{1/2}$ (*ca.* 50 mV/log [H_2O]) suggests strongly that an increase of the number of anion radicals solvated by water facilitates the rate of coupling between the anion radicals because of a decrease in the coulombic repulsive force between two anion radicals.

To examine whether or not the reactions (Eqs. 1—3) are applicable in the solution containing a low concentration (7.5%) of water, the voltammograms for the reduction of **1** were also measured by changing the experimental parameters. In the 7.5% water–ethanol solution, results similar to those obtained in the 50% water–ethanol solution were obtained. That is, the plots of log $[i^{2/3}/(i_d-i)]$ *vs.* E showed a straight line having a slope of 53 mV, and the dependences of $E_{1/2}$ on both ω and C, $\partial E_{1/2}/\partial \log \omega$ and $\partial E_{1/2}/\partial \log C$, were −25 and 20 mV, respectively. Thus, we concluded that no serious change in the mechanism occurred in the water concentration range tested.

The dl/meso *Ratio of the Products.* To give further experimental support for the formation of the solvated anion radical, the variation of isomer ratio (*dl*/*meso*) of **2** was examined. On steric grounds, when the water concentration is high enough to solvate all anion radicals, the most favorable conformation in the transition state of the dimerization reaction is I, whereas when a part of the radicals are solvated, structure II is more attractive than I because of the aid of inter-radical hydrogen bonding.

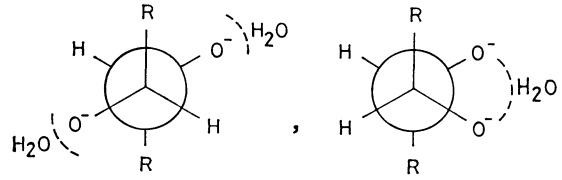

where R=$-C_6H_4N(CH_3)_2$.

TABLE 1. ISOMER RATIOS IN REDUCTION PRODUCTS OF **1**

Run	Solvent[a)]	Amount of **1** g	Amount of **1** (mM)	Charge passed mF	Yield of product (**2**) *meso* g	Yield of product (**2**) *dl* g	Ratio of *dl*/*meso*	Total yield of product %
1	50% H_2O + 50% EtOH	1.0045	(67.0)	6.57	0.38	0.32	0.84	70
2		1.0090	(67.3)	6.57	0.38	0.31	0.82	68
3		1.0011	(66.7)	6.57	0.38	0.30	0.79	68
							Av 0.82	
4	5% H_2O + 95% EtOH	1.0236	(69.4)	6.94	0.23	0.45	2.0	66
5		1.0116	(67.3)	8.66	0.28	0.44	1.6	71
6		1.0044	(67.0)	6.58	0.24	0.47	2.0	71
							Av 1.9	

a) The volume of all solutions was 100 ml.

Thus, the *dl*/*meso* ratio of the products must increase with a decrease in the concentration of water. According to the macroscale electrolysis data obtained (Table 1), the *dl*/*meso* ratio changed from 0.8 in the 50% water–ethanol solution to 1.9 in the 5% water–ethanol solution. In the latter case, the current decreased to less than one-tenth of the current in the former case at the same cathode potential, −1.8 V *vs.* SCE; this is because the rate of dimerization decreased with decreasing water concentration, as will be described later. The result of the *dl*/*meso* ratio is consistent with the above consideration about the formation of the solvated anion radical.

For some aromatic aldehydes, the DIM II mechanism which was rejected in the present experiment for **1** has been proposed in aqueous basic solutions. This unusual behavior for **1** is probably because the electron density on the oxygen atom of the carbonyl group is high, due to the extremely strong electron-donating effect of the *N*,*N*-dimethylamino group, and thus the hydrogen bonding with a water molecule is facilitated. To clarify the structure of the anion radical and the mechanism of the solvation, further experiments are required.

TABLE 2. RATE CONSTANT CALCULATED FROM Eq. 4

Concentration of Water[a)] vol %	**1** mM	log ω_0	ω_0 rad s^{-1}	k[b)] M^{-1} s^{-1}
50	1.19	2.70	501.2	2.21×10^4
50	0.406	2.34	218.8	2.38
				Av 2.5×10^4
15	9.31	2.38	239.9	1.4×10^3
7.5	10.0	2.25	177.8	9.6×10^3

a) Water–ethanol solution containing 1 M NaOH.
b) For the calculation, the diffusion coefficient (D) of **1** and the kinematic viscosity of the solution obtained for each solution were used.

Rate of the Dimerization. The rate constant of the dimerization (k) can be estimated from the variation of $E_{1/2}$ with log ω.[2] The value of ω at the intersection of the oblique linear part of the $E_{1/2}$—log ω plots with the horizontal part, ω_0, gives

$$(1/3)kC(\delta^2/D) = 1, \tag{4}$$

where $\delta = 1.61\ D^{1/3}\nu^{1/6}\omega_0^{-1/2}$.

As can be seen in Fig. 2, an intersection in the $E_{1/2}$—log ω plots is observed for the concentrations of **1** lower than 1.2 mM in 50% water–ethanol solutions containing 1 M NaOH. Thus the apparent rate constant for the dimerization is calculated to be 2.5×10^4 M^{-1} s^{-1} by using Eq. 4 (Table 2), where the value of k obtained is the total value of the rate constants for the two reactions of R^- to both *dl* and *meso* types of **2**. When the water concentration decreased, the intersection in $E_{1/2}$—log ω plots was observed even in the solution containing 10 mM of **1** (Fig. 5); this is because the rate of dimerization decreased. For 7.5 and 15% water–ethanol solutions, the values of k thus obtained are listed in Table 2. The decrease in the k value at low concentrations of water indicates that an increase in the coulombic repulsive force between the anion radicals lowered the rate of the dimerization.

The authors wish to express their thanks to Associate Professor Tsutomu Nonaka of Tokyo Institute of Technology for his useful advice.

Appendix

Let us consider the following reactions:

$$A + ne \rightleftarrows B \text{ (reversible)}$$

$$2B \xrightarrow{k} B_2 \text{ (irreversible fast dimerization)}$$

At the steady state, the boundary value problem of the above reactions at an RDE can be formulated as follows, under the usual experimental conditions:

$$D_A\frac{d^2A}{dx^2} - V_x\frac{dA}{dx} = 0, \tag{1}$$

$$D_B\frac{d^2B}{dx^2} - V_x\frac{dB}{dx} - kB^2 = 0, \tag{2}$$

where $V_x = -0.51\ \omega^{3/2}\nu^{-1/2}x^2$, with the boundary conditions of

$$x = 0\text{: } A = A_0,\ B = B_0, \text{ and } D\frac{dA}{dx} = -D\frac{dB}{dx} = \frac{i}{nF}$$

$$(D_A = D_B = D \text{ is assumed}), \tag{3}$$

$$x \to \infty\text{: } A = A^*, \text{ and } B = 0, \tag{4}$$

where A^* is the bulk concentration of A, and A_0 and B_0 are, respectively, the concentrations of A and B at the surface of the RDE. The symbols used without definition have their ordinary meanings.[10]

The solution of Eq. 1 is

$$A = A_0 + (A^*-A_0)\frac{\int_0^x \exp\left(\int_0^x \frac{V_x}{D}dx\right)dx}{\int_0^\infty \exp\left(\int_0^\infty \frac{V_x}{D}dx\right)dx}, \quad (5)$$

and the concentration gradient of A at the electrode surface is

$$\left(\frac{dA}{dx}\right)_{x=0} = \frac{A^*-A_0}{\int_0^\infty \exp\left(\int_0^\infty \frac{V_x}{D}dx\right)dx}, \quad (6)$$

and thus the current density (i) is represented by

$$i = nFD\left(\frac{dA}{dx}\right)_{x=0} = nFD(A^*-A_0)/\delta \quad (7)$$

where $\delta = 1.61\, D^{1/3}\, \nu^{1/6}\, \omega^{-1/2}$.

By using the limiting current, i_d ($A_0=0$ in Eq. 7), we obtain

$$A_0 = \left(\frac{i_d-i}{nFD}\right)\delta. \quad (8)$$

On the other hand, Eq. 2 can not be solved analytically, but we may use the simplified model.[11] Here, let us neglect the second term in Eq. 2; thus we obtain

$$D\frac{d^2B}{dx^2} - kB^2 = 0. \quad (9)$$

After satisfying the boundary conditions, we obtain the solution of Eq. 9:

$$B = \frac{6D/k}{(\sqrt{6D/(kB_0)}+x)^2}, \quad (10)$$

Thus, the current is

$$i = -nFD\left(\frac{dB}{dx}\right)_{x=0} = (nFD)^{3/2}B_0^{3/2}/\varepsilon \quad (11)$$

where $\varepsilon = (3/2)^{1/3}\, (nF)^{1/3}\, D^{2/3}\, k^{-1/3}$,
and we obtain

$$B_0 = \left(\frac{i^{2/3}}{nFD}\right)\varepsilon. \quad (12)$$

Under the condition of the Nernst equation holding for the electron transfer reaction (A+n e$\rightleftarrows$B), we obtain

$$\begin{aligned} E &= E_0 - \frac{RT}{nF}\ln\frac{B_0}{A_0} \\ &= E_0 - \frac{RT}{nF}\ln\frac{i^{2/3}}{(i_d-i)}\frac{\varepsilon}{\delta} \\ &= E_0 - \frac{RT}{nF}\ln\frac{\varepsilon}{\delta} - \frac{RT}{nF}\ln\frac{i^{2/3}}{(i_d-i)}. \end{aligned} \quad (13)$$

By substituting $i=(1/2)i_d$ and $i_d = nFDA^*/\delta$ into Eq. 13, we get the half-wave potential:

$$\begin{aligned} E_{1/2} &= E_0 - \frac{RT}{nF}\ln\frac{2^{1/3}\varepsilon}{i_d^{1/3}\delta} \\ &= E_0 - \frac{RT}{nF}\ln\frac{3^{1/3}D^{1/3}k^{-1/3}A^{*-1/3}}{\delta^{2/3}} \\ &= E_0 - \frac{RT}{3nF}\ln\frac{3D}{kA^*\delta^2} \end{aligned} \quad (14\text{-}1)$$

or

$$= E_0 - \frac{RT}{3nF}\ln\frac{3D^{1/3}}{1.61^2\nu^{1/3}} + \frac{RT}{3nF}\ln\frac{kA^*}{\omega}. \quad (14\text{-}2)$$

Equations 13 and 14 obtained here are the same as those derived by other workers,[2,12] and were used in the present work.

References

1) C. P. Andrieux, L. Nadjo, and J. M. Saveant, *J. Electroanal. Chem. Interfacial Electrochem.*, **42**, 223 (1973).
2) L. Nadjo and J. M. Saveant, *J. Electroanal. Chem. Interfacial Electrochem.*, **44**, 327 (1973).
3) M. J. Allen, *J. Org. Chem.*, **15**, 435 (1950).
4) I. Taniguchi and T. Sekine, *Denki Kagaku*, **43**, 201 (1975); I. Taniguchi, A. Yoshiyama, and T. Sekine, *ibid.*, **45**, 442 (1977).
5) J. A. Stocker and D. H. Kern, *J. Org. Chem.*, **33**, 1271 (1968).
6) L. Nadjo and J. M. Saveant, *J. Electroanal. Chem. Interfacial Electrochem.*, **33**, 419 (1971).
7) M. Lipsztajn, T. M. Krygowski, and Z. Galus, *J. Electroanal. Chem. Interfacial Electrochem.*. **49**, 17 (1974).
8) L. A. Avaca and A. Bewick, *J. Electroanal. Chem. Interfacial Electrochem.*, **41**, 405 (1973).
9) E. Lamy, L. Nadjo, and J. M. Saveant, *J. Electroanal. Chem. Interfacial Electrochem.*, **50**, 141 (1974).
10) V. G. Levich, "Physicochemical Hydrodynamics," Prentice-Hall Inc., Englewood Cliffs, New Jersey (1962), Chap. 2.
11) L. K. J. Tong, K. Liang, and W. R. Ruby, *J. Electroanal. Chem. Interfacial Electrochem.*, **13**, 245 (1967).
12) R. Bonnaterre and G. Cauquis, *J. Electroanal. Chem. Interfacial Electrochem.*, **33**, 199 (1971).